doi:10.1093/brain/aws082 Brain 2012: 135; 1622–1638 | 1622

BRAIN
A JOURNAL OF NEUROLOGY

Immunopathology of autoantibody-associated encephalitides: clues for pathogenesis

Christian G. Bien,[1] Angela Vincent,[2] Michael H. Barnett,[3] Albert J. Becker,[4] Ingmar Blümcke,[5] Francesc Graus,[6] Kurt A. Jellinger,[7] David E. Reuss,[8] Teresa Ribalta,[9] Jürgen Schlegel,[10] Ian Sutton,[11] Hans Lassmann[12] and Jan Bauer[12]

1 Epilepsy Centre Bethel, Krankenhaus Mara, 33617 Bielefeld, Germany
2 Department of Clinical Neurology, Weatherall Institute of Molecular Medicine, John Radcliffe Hospital, Oxford OX3 9DS, UK
3 Institute of Clinical Neurosciences, Royal Prince Alfred Hospital, Brain and Mind Research Institute, Sydney, Australia
4 Department of Neuropathology, University of Bonn Medical Centre, 53127 Bonn, Germany
5 Department of Neuropathology, Friedrich-Alexander-University Erlangen-Nuremberg, 91054 Erlangen, Germany
6 Service of Neurology, Hospital Clinic, Institut d'Investigació Biomèdica August Pi i Sunyer (IDIBAPS), Universitat de Barcelona, 08036 Barcelona, Spain
7 Institute of Clinical Neurobiology, Medical University of Vienna, A-1090 Vienna, Austria
8 Department of Neuropathology, University Hospital Heidelberg and German Cancer Centre (DKFZ), 69120 Heidelberg, Germany
9 Department of Pathology, Institut d'Investigació Biomèdica August Pi i Sunyer (IDIBAPS), Hospital Clinic, Universitat de Barcelona, 08036 Barcelona, Spain
10 Division of Neuropathology, Institute of Pathology, Technical University, 81675 Munich, Germany
11 Department of Neurology, St Vincent's Hospital, Victoria Street, Darlinghurst Sydney 2010, Australia
12 Department of Neuroimmunology, Centre for Brain Research, Medical University of Vienna, A-1090 Vienna, Austria

Correspondence to: Dr Jan Bauer,
Centre for Brain Research,
Medical University of Vienna,
Spitalgasse 4,
A-1090 Vienna, Austria
E-mail: jan.bauer@meduniwien.ac.at

Classical paraneoplastic encephalitis syndromes with 'onconeural' antibodies directed to intracellular antigens, and the recently described paraneoplastic or non-paraneoplastic encephalitides and antibodies against both neural surface antigens (voltage-gated potassium channel-complexes, *N*-methyl-D-aspartate receptors) and intracellular antigens (glutamic acid decarboxylase-65), constitute an increasingly recognized group of immune-mediated brain diseases. Evidence for specific immune mechanisms, however, is scarce. Here, we report qualitative and quantitative immunopathology in brain tissue (biopsy or autopsy material) of 17 cases with encephalitis and antibodies to either intracellular (Hu, Ma2, glutamic acid decarboxylase) or surface antigenic targets (voltage-gated potassium channel-complex or *N*-methyl-D-aspartate receptors). We hypothesized that the encephalitides with antibodies against intracellular antigens (intracellular antigen-onconeural and intracellular antigen-glutamic acid decarboxylase groups) would show neurodegeneration mediated by T cell cytotoxicity and the encephalitides with antibodies against surface antigens would be antibody-mediated and would show less T cell involvement. We found a higher CD8/CD3 ratio and more frequent appositions of granzyme-B$^+$ cytotoxic T cells to neurons, with associated neuronal loss, in the intracellular antigen-onconeural group (anti-Hu and anti-Ma2 cases) compared to the patients with surface antigens (anti-*N*-methyl-D-aspartate receptors and anti-voltage-gated potassium channel complex cases). One of the glutamic acid decarboxylase antibody encephalitis cases (intracellular antigen-glutamic acid decarboxylase group) showed multiple appositions of GrB-positive T cells to neurons. Generally, however, the glutamic acid decarboxylase antibody cases showed less

Received August 22, 2011. Revised December 22, 2011. Accepted February 5, 2012. Advance Access publication April 25, 2012

intense inflammation and also had relatively low CD8/CD3 ratios compared with the intracellular antigen-onconeural cases. Conversely, we found complement C9neo deposition on neurons associated with acute neuronal cell death in the surface antigen group only, specifically in the voltage-gated potassium channel-complex antibody patients. *N*-methyl-D-aspartate receptors-antibody cases showed no evidence of antibody and complement-mediated tissue injury and were distinguished from all other encephalitides by the absence of clear neuronal pathology and a low density of inflammatory cells. Although tissue samples varied in location and in the stage of disease, our findings strongly support a central role for T cell-mediated neuronal cytotoxicity in encephalitides with antibodies against intracellular antigens. In voltage-gated potassium channel-complex encephalitis, a subset of the surface antigen antibody encephalitides, an antibody- and complement-mediated immune response appears to be responsible for neuronal loss and cerebral atrophy; the apparent absence of these mechanisms in *N*-methyl-D-aspartate receptors antibody encephalitis is intriguing and requires further study.

Keywords: encephalitis; antibodies; pathogenic; cytotoxic T lymphocytes; complement

Abbreviations: CASPR2 = contactin-associated protein-2; GAD = glutamic acid decarboxylase; GrB = granzyme-B; IAg = intracellular antigen; LGI1 = leucin-rich, glioma inactivated protein-1; MAP2 = microtubule associated protein-2; MHC = major histocompatibility complex; NeuN = neuronal nuclei; NMDAR = N-methyl-d-aspartate receptor; TUNEL = terminal deoxynucleotidyl transferase dUTP nick end labelling; VGKC = voltage-gated potassium channel

Introduction

In recent years the spectrum of chronic inflammatory brain diseases characterized by the presence of antigen-specific antibodies in serum and CSF has greatly expanded. More and more, cases such as glutamic acid decarboxylase (GAD)-65 antibody encephalitis (Malter *et al*., 2010), voltage-gated potassium channel (VGKC) complex antibody encephalitis (Irani *et al*., 2010*a*), *N*-methyl-D-aspartate receptor (NMDAR) antibody encephalitis (Dalmau *et al*., 2008) or the most recent α-amino-3-hydroxy-5-methyl-4-isoxazolepropionic acid (AMPA) receptor (Lai *et al*., 2009) or gamma aminobutyric acid receptor GABA(B) antibody encephalitides (Lancaster *et al*., 2010) are recognized. In clinico-topological terms, the entities are designated as limbic encephalitis, cerebellar degeneration, brainstem encephalitis or encephalomyelitis. Furthermore, these syndromes can be grouped into paraneoplastic and non-paraneoplastic conditions. Paraneoplastic syndromes have received much of the attention since their conceptualization in the mid-20th century. Approximately 60% of patients with these syndromes have serum and CSF antibodies to intracellular antigens, often even intranuclear antigens such as Hu, Ma, Yo or amphiphysin (Saiz *et al*., 1999; Graus *et al*., 2001; Dalmau and Rosenfeld, 2008). A certain number of these paraneoplastic cases, however, have antibodies against surface antigens such as the NMDAR (Dalmau *et al*., 2011), the metabotropic glutamate receptor 1 (Dalmau and Rosenfeld, 2008; Lai *et al*., 2009; Lancaster *et al*., 2011) or the metabotropic glutamate receptor 5 (Lancaster *et al*., 2011).

The clinical syndromes are important entry points for the diagnostic work-up of patients, and the detection of a potential underlying cancer may be essential for a patient's prognosis *quoad vitam*. It has been suggested, however, that the most important determinant of the underlying immunopathogenesis and responsiveness to immunosuppression is the antibody status of the affected individual, which may determine the response to treatment (Dalmau and Rosenfeld, 2008; Graus *et al*., 2010; Vincent *et al*., 2010). Specifically, striking differences have been suggested between disorders with intracellular antigens versus those with antibodies to neural surface antigens. Disorders with antibodies to intracellular antigens are considered poorly responsive to immunotherapy (Vincent *et al*., 1999; Dalmau and Rosenfeld, 2008; Malter *et al*., 2010) and may be mediated by cytotoxic T cells (Bernal *et al*., 2002; Dalmau and Rosenfeld, 2008). Therefore, although of diagnostic importance, the antibodies against intracellular antigens are considered an immunological epiphenomenon (Dalmau and Rosenfeld, 2008; Graus *et al*., 2010). On the other hand, disorders associated with surface antigens, such as encephalitis with antibodies to the VGKC-complex or NMDAR, often respond well to treatment (Vincent *et al*., 2004; Malter *et al*., 2010; Dalmau *et al*., 2011) and may be mediated by antibody-binding, internalization and loss of the target surface antigens (Hughes *et al*., 2010). But many questions remain unresolved. For instance, why do patients with antibodies to the VGKC-complex, despite clinical improvements in mental function and often complete seizure control, develop medial temporal lobe and sometimes more global, atrophy (Vincent *et al*., 2004; Soeder *et al*., 2005)? Why is this atrophy not seen or is reversible in patients with NMDAR antibodies, despite their often devastating primary illness and frequent association with ovarian teratomata (Iizuka *et al*., 2010; Dalmau *et al*., 2011)? Furthermore, how does one classify patients with GAD antibodies directed to an intracellular antigen, but usually not paraneoplastic in origin, who suffer from limbic encephalitis or chronic temporal lobe epilepsy (Malter *et al*., 2010)?

Immunopathological analysis of the various antibody-associated encephalitides may help to elucidate the underlying immunopathogenic mechanisms, but unfortunately the published studies are scarce, there is a lack of quantitative data and, to date, there are no studies correlating brain immunopathology with antibody status. Here, rather than comparing paraneoplastic with non-paraneoplastic encephalitis, we first investigated the hypothesis that cases with intracellular antigen antibodies show a different immune reaction than that of cases with surface antigen antibodies (Vincent *et al*., 1999; Dalmau and Rosenfeld, 2008; Graus *et al*., 2010). More specifically, we sought evidence that T cells

would play a cytotoxic role in the cases with intracellular antigen antibodies, and that antibody and/or complement-mediated mechanisms are responsible for neurodegeneration in encephalitides with surface antigen antibodies. Secondly, we thoroughly analysed and compared the immunopathology of tissue from patients with GAD, VGKC-complex and NMDAR antibodies. Our results reveal that paraneoplastic cases with antibodies to intracellular antigens, as well as the non-paraneoplastic GAD65 cases, show signs of a T cell-mediated immune response. In the VGKC-complex cases with antibodies to surface antigens, we found antibody- and complement-mediated destruction of neurons. Finally, the NMDAR cases showed neither a cytotoxic T cell attack nor indication of complement-mediated neuronal damage. Clinically, our results may help to rationalize immunological treatment choices for these disorders.

Materials and methods

Patients

Paraffin-embedded brain specimens of 17 patients were studied. Individual patients are labelled according to the respective antibody and number (Hu/1, Hu/2, Hu/3, etc.). The specimens were obtained between 1991 and 2009 during autopsy ($n = 6$), epilepsy surgery ($n = 5$), diagnostic open brain biopsy ($n = 5$) or diagnostic stereotactic brain biopsy ($n = 1$). Biopsy sites were chosen according to abnormal areas on brain MRI. In patients with anti-NMDAR encephalitis (who all had normal MRI), the biopsy site chosen was based on maximal EEG abnormalities (as in Patient NMDAR1) or (in cases with diffusely abnormal EEG) by neurosurgical considerations in the right frontal convexity. Mean disease duration at specimen collection was 21 months (SD ± 37 months). Epilepsy surgery procedures were aimed at resection of the hypothesized epileptogenic area.

Serum antibodies were determined by standard methods (Vedeler *et al*., 2006) using a combination of immunohistochemistry and blot techniques. For GAD and NMDAR antibodies, titration of indirect immunohistochemistry, and for VGKC-complex antibodies radioimmunoprecipitation with ^{125}I-labelled dendrotoxin-VGKC-complexes, was used to quantitate antibody concentration. From 2/4 VGKC-complex antibody$^+$ patients, serum for leucin-rich, glioma inactivated protein-1 (LGI1) and contactin-associated protein-2 (CASPR2) antibody subtyping was available when these antibody tests were established (Irani *et al*., 2010*a*). No quantitative data were obtained for onconeural antibodies and LGI1/CASPR2 antibodies. Patients harboured antibodies to the following antigens: Hu ($n = 4$), Ma2 ($n = 3$), GAD ($n = 3$), VGKC-complex ($n = 4$, in one directed to LGI1, in one neither directed to LGI1 nor to CASPR2) and NMDAR ($n = 3$).

Here we divided our patients into three groups. An intracellular antigen (IAg)-onconeural group which consists of the anti-Hu and anti-Ma2 cases, an IAg-GAD group, which holds the three non-paraneoplastic anti-GAD cases, and a surface antigen group, which contains both the anti-NMDAR and anti-VGKC cases. Demographic and paraclinical data of the individual patients are presented in Table 1. As positive controls for a specific cytotoxic T cell reaction, we studied 22 cases of Rasmussen encephalitis (Bien *et al*., 2002; Bauer *et al*., 2007; Schwab *et al*., 2009). In addition, we used neurodegenerative controls; 15 cases of Ammon's horn sclerosis in patients operated on for mediotemporal epilepsy (Wieser and ILAE commission on neurosurgery for epilepsy, 2004), five cases of Alzheimer disease and five cases of acute cerebral hypoxia. Finally, autopsy controls without known neurological disease ($n = 7$) were included. For evaluation of NMDAR density, we compared biopsies from patients with anti-NMDAR encephalitis to surgical specimens from five patients with non-lesional epilepsy (temporal and extratemporal specimens). For immunoglobulin and C9neo deposition we used spinal cord sections of a patient with neuromyelitis optica with anti-aquaporin-4 antibodies as positive control.

Histochemistry and immunohistochemistry

Sections (4 μm) of paraffin embedded specimens were routinely stained with haematoxylin and eosin, Nissl stain for neurons and Luxol fast blue for myelin. Immunohistochemical staining and confocal fluorescence double staining were performed according to previously published protocols (Bien *et al*., 2002; Bauer *et al*., 2007) using the primary antibodies listed in Supplementary Table 1. As a first step, a qualitative assessment of the basic pathology, aimed at identifying the cell types (neurons, astrocytes, oligodendrocytes) that are lost or damaged, was undertaken. Immune reactions within tissues were then studied by both qualitative and quantitative methods using markers that identify inflammatory cells (T cells, B cells, plasma cells, macrophages and microglia), immunoglobulins, complement and major histocompatibility complex (MHC) molecules. For the CD3, CD8, MHC class I and GrB stainings, biotinylated tyramine enhancement was used as described previously (Bien *et al*., 2002).

Confocal laser fluorescence microscopy

Fluorescence immunohistochemistry was performed on paraffin sections as described for light microscopy with few modifications. For confocal fluorescent double labelling with primary antibodies from different species, antibodies were applied simultaneously at 4°C overnight. After washing with Dako washing buffer (DakoCytomation), secondary antibodies consisting of donkey anti-mouse Cy3 (Jackson ImmunoResearch, 1:200) and biotinylated donkey anti-rabbit (Amersham Pharmacia Biotech; 1:200) were applied simultaneously for 1 h at room temperature, followed by application of streptavidin-Cy2 (Jackson ImmunoResearch; 1:75) for 1 h at room temperature. Fluorescent preparations were then stained with 4′,6′-diamidino-2-phenylindole (DAPI, Sigma), embedded and examined using a confocal laser scan microscope (Leica SP5) equipped with lasers for 504, 488, 543 and 633 nm excitation. Scanning for DAPI (504 nm), Cy2 (488 nm) and Cy3 (543 nm) was performed sequentially to rule out fluorescence bleed-through.

Assessment of cell loss

Chronic cell loss was qualitatively assessed in microtubule associated protein-2 (MAP2)/neuronal nuclei (NeuN) stained sections. The presence of axonal spheroids and excessive neuronal cytoplasmic accumulation of amyloid precursor protein (suggesting disruption of axonal protein transport) was qualitatively assessed by amyloid precursor protein immunostaining. Brain MRIs, which were available in 10/17 patients, were visually evaluated for signs of tissue loss.

TUNEL

In order to detect cells with DNA fragmentation, terminal deoxynucleotidyl transferase dUTP nick end labelling (TUNEL) was performed

Table 1 Demographic data of the patients

Patient[a]	Gender	Age[b]	Antibody directed to (antibodies tested)	Tumour	Clinical syndrome	Disease duration (months)	Cause of death	Immunotreatment prior to specimen collection	CSF (i) Time to brain tissue collection (ii) Cell count (iii) Protein (iv) Unmatched oligoclonal bands	Specimen collection	Tissues	Brain atrophy on follow-up brain MRI
IAg-onconeural group (intracellular antigen antibodies)												
Ma2/1 (Barnett *et al.*, 2001)	F	71	**Ma2** (onco, GAD)	Adeno-carcinoma lung	PEM	7	Death 1 week after seizure series	Plasma exchange briefly	(i) −5 mo (ii) 4/μl (iii) 0.83 g/l (iv) Negative	Autopsy	Brainstem, hippocampus, cerebellum	n.a.
Ma2/2	M	36	**Ma2** (onco)	Testicular carcinoma	PLE	1	–	None	(i) −1 mo (ii) 9/μl (iii) <0.5 g/l (iv) Negative	Stereotactic biopsy	Entorhinal cortex	Yes, mediotemporal (Fig. 1)
Ma2/3	M	34	**Ma2** (onco)	Testicular carcinoma	PLE	9	–	None	(i) −2 mo (ii) 15/μl (iii) 0.39 g/l (iv) Positive	Epilepsy surgery	Hippocampus	n.a.
Hu/1	M	65	**Hu** (onco)	SCLC	PEM	13	n.a.	Unknown	n.a.	Autopsy	Basal ganglia, cerebellum	n.a.
Hu/2 (Bernal *et al.*, 2002)	M	58	**Hu** (onco)	Oatcell carcinoma lung	PEM	2.5	Progression of neurological syndrome, infectious complications and death from sepsis	Plasma exchange 1 month before death	(i) −3 mo (ii) 0 (iii) 0.76 g/l (iv) n.a.	Autopsy	Brainstem	n.a.
Hu/3 (Bernal *et al.*, 2002)	M	49	**Hu** (onco)	Adeno carcinoma prostata	PEM	1.5	Progression of neurological syndrome, infectious complications and death from sepsis	IVIG 2 g/kg and IVMP 3 g within 1 month prior to death	(i) −10 days (ii) 20/μl (iii) 1.28 g/l (iv) n.a.	Autopsy (as Hu/2)	Medulla oblongata	n.a.
Hu/4 (Bernal *et al.*, 2002)	F	53	**Hu** (onco)	Oatcell carcinoma lung	PEM	11	Progression of neurological syndrome, infectious complications and death from sepsis	IVIG 2 g/kg and IVMP 3 g within 1 month prior to death	(i) −5 mo (ii) 0 (iii) 0.45 (iv) N.a.	Autopsy (as Hu/2)	Cortex	n.a.
Summary, means ± SD	2/7 F		4 Hu, 3 Ma2			6 ± 4		4/7	(i) −2.7 ± 1.8 mo (ii) 8 ± 8/μl, abnormal 3/6 (iii) 0.74 ± 0.32 g/l, abnormal 3/6 (iv) 1/3 positive			*1/1 yes*
IAg-GAD group (GAD antibodies)												
GAD/1	F	18	**GAD 1:16 000** (onco, GAD, VGKC)	None	LE	127	–	None	(i) +10 years (ii) 1/μl (iii) 0.43 g/l (iv) positive	Epilepsy surgery	Hippocampus	No
GAD/2	M	31	**GAD 1:1000** (onco, GAD)	None	LE	115	–	None	(i) +20 days (ii) 25/μl (iii) 0.93 g/l (iv) Negative	Epilepsy surgery	Hippocampus	Yes, mediotemporal
GAD/3 [Case vignette in Bien *et al.* (2007)]	F	24	**GAD 1:32 000** (onco, GAD, VGKC)	None	LE	7	–	None	(i) −1 mo (ii) 10/μl (iii) 0.33 g/l (iv) Positive	Epilepsy surgery	Hippocampus	Yes, mediotemporal (Fig. 1)

(continued)

Table 1 Continued

Patient[a]	Gender	Age[b]	Antibody directed to (antibodies tested)	Tumour	Clinical syndrome	Disease duration (months)	Cause of death	Immunotreatment prior to specimen collection	CSF (i) Time to brain tissue collection (ii) Cell count (iii) Protein (iv) Unmatched oligoclonal bands	Specimen collection	Tissues	Brain atrophy on follow-up brain MRI
Summary, means ± SD	2/3 F	24 ± 5	3 GAD	None		83 ± 54		0/3	(i) 41 ± 56 mo (ii) 12 ± 10/μl, abnormal2/3 (iii) 0.56 ± 0.26 g/l, abnormal1/3 (iv) 2/3 positive			2/3 yes
SAg group (surface antigen antibodies)												
VGKC/1 [Case 10 in Vincent *et al.* (2004)]	M	56	VGKC 2224 pmol/l; LGI1$^+$, CASPR2$^-$ (onco, GAD, VGKC)	None	LE	8	–	None	(i) −2 wks (ii) 6/μl (iii) 0.51 g/l (iv) Negative	Open biopsy	Uncus	Yes, global with mediotemporal accentuation (Fig. 1)
VGKC/2	M	59	VGKC 958 pmol/l; LGI1, CASPR2 ab status unknown (VGKC)	None	LE	5	Acute bronchopneumonia	Unknown	(i) −2 mo (ii) 0 (iii) 0.52 (iv) n.d.	Autopsy	Hippocampus	n.a.
VGKC/3	M	33	VGKC 167 pmol/l; LGI1$^-$, CASPR2$^-$ (onco, VGKC)	None	Multifocal encephalitis	9	–	None	(i) −2 wks (ii) 18/μl (iii) 0.71 g/l (iv) Positive	Open biopsy	Uncus	Yes, global (Fig. 1)
VGKC/4	F	68	VGKC 288 pmol/l; LGI1, CASPR2 antibody status unknown (onco, GAD, VGKC)	None	LE	8	–	None	(i) 4 mo (ii) 2/μl (iii) 0.33 g/l (iv) negative	Epilepsy surgery	Amygdala	n.a.
NMDAR/1 (Niehusmann *et al.*, 2009)	M	22	NMDAR 1:500 (onco, GAD, VGKC, NMDAR)	None	Encephalopathy	2	–	None	(i) $^+$8 mo (ii) 1/μl (iii) 0.29 g/l (iv) Negative	Open biopsy	Temporal neocortex	No (Fig. 1)
NMDAR/2 (Niehusmann *et al.*, 2009)	F	17	NMDAR 1:2000 (onco, GAD, VGKC, NMDAR)	None	Encephalopathy	12 (from onset of first disease bout; 2.2 mo after onset of first relapse)	–	1 week course of dexamethasone 1 mo before biopsy	(i) −4 mo (ii) 1/μl (iii) 0.19 g/l (iv) Positive	Open biopsy	Frontal lobe	No
NMDAR/3	F	26	NMDAR 1:2000 (onco, GAD, VGKC, NMDAR)	None	Encephalopathy	11	–	60 mg prednisone and 150 mg azathioprin at time of biopsy	(i) −24 days (ii) 13/μl (iii) 0.31 g/l (iv) Positive	Open biopsy	Frontal lobe	No
Summary, means ± SD	3/7 F	40 ± 19	4 VGKC, 3 NMDAR			9 ± 6		2/6	(i) 1.0 ± 1.8 mo (ii) 7 ± 7/μl, abnormal 3/6 (iii) 0.39 ± 0.17 g/l, abnormal 2/6 (iv) 3/6 positive			VGKC: 3/3 NMDAR: 0/3
Control groups												
Rasmussen encephalitis, $n = 22$	13/22 F	16 ± 12	n.a.	None		53 ± 33			n.a.	Epilepsy surgery ($n = 9$), biopsy ($n = 13$)	Temporal ($n = 15$), extratemporal ($n = 7$)	Yes
Neurodegeneration, $n = 25$	12/25 F	47 ± 26	n.a.	None		129 ± 190 (without Alzheimer cases)			n.a.		Hippocampi	n.a.

(continued)

Table 1 Continued

Patient[a]	Gender	Age[b]	Antibody directed to (antibodies tested)	Tumour	Clinical syndrome	Disease duration (months)	Cause of death	Immunotreatment prior to specimen collection	CSF (i) Time to brain tissue collection (ii) Cell count (iii) Protein (iv) Unmatched oligoclonal bands	Specimen collection	Tissues	Brain atrophy on follow-up brain MRI
(AHS, $n = 15$; Alzheimer, $n = 5$, acute hypoxia, $n = 5$)										Autopsy (Alzheimer, hypoxia) or epilepsy surgery (AHS)		
Normal controls, $n = 7$	3/7 F	59 ± 10	n.a.	None		–			n.a.	Autopsy	Hippocampi	n.a.

a With references to papers in which cases has been included previously.
b Age and disease durations were not significantly different between the IAg-onconeural, IAg-GAD and surface antigen group. The following CSF parameters were considered abnormal: cell count >5/µl, protein content >0.5 g/l. Means ± SD.
AHS = Ammon's horn sclerosis; IVIG = intravenous immunoglobulins; IVMP = intravenous methylprednisolone; LE = limbic encephalitis; mo = months; PEM = paraneoplastic encephalomyelitis; PLE = paraneoplastic limbic encephalitis; SCLC = small cell lung carcinoma; n.a. = not applicable; F = female; M = male.

with the *In Situ* Cell Death Detection Kit (alkaline phosphatase) from Roche. Briefly, 3–5 µm paraffin sections were deparaffinized, treated with chloroform and air dried. Next, sections were treated with 0.1% protease for 30 min at 37°C. This was followed by incubation with labelled dUTP in the presence of terminal transferase according to the manufacturer's guidelines. Sections were developed with fast blue. Subsequently, the sections were stained with MAP2 or NeuN, or a mixture of both, followed by horseradish peroxidase-conjugated anti-mouse as a secondary system. This staining was developed with amino-ethyl carbazole as substrate. As a result, DNA fragmentation in the nucleus appears blue while MAP2/NeuN proteins appear red.

Quantification of cells

Quantification of parenchymal $CD3^+$, $CD8^+$, granzyme-B $(GrB)^+$, $CD20^+$, $CD138^+$ and $CD68^+$ cells in tissue regions exhibiting inflammation on haematoxylin and eosin-stained sections was performed in consecutive sections using an ocular morphometric grid covering an area of 1 mm^2 at ×100 (GrB^+ cells were assessed at ×400 to be able to see the small granular signal). Scoring was performed by an experienced blinded observer (J.B.). The evaluated areas had a mean size of 10.8 mm^2 [range 0.5 mm^2 (in the only stereotactically obtained specimen, Patient 5)—50.0 mm^2] per specimen. The $CD8^+/CD3^+$, $GrB^+/CD3^+$ and macrophage/microglia ratios (differentiated according to cell body morphology of $CD68^+$ cells) were calculated by determining the cell density of the respective stainings in corresponding regions of consecutive sections. In addition to the CD8/CD3 ratio in the parenchyma we also calculated this ratio in the perivascular space of blood vessels (perivascular cuffs). For this, we counted the number of CD3 and CD8 T cells (on average ~200 cells) in blood vessels of consecutive sections.

Statistics

For metric data, a Kruskal–Wallis followed by Dunn's Multiple Comparisons Test was used. For categorical data, Fisher's exact test was used. A *P*-value of <0.05 was considered significant. All tests were performed with Graphpad Prism 5.0 (GraphPad Software, Inc.).

Results

Brain specimens

We studied brain material of 17 patients (10 male, 7 female, 17–71 years old). In Table 1, the clinical diagnoses, associated tumours and site of the specimens are grouped according to the antibody status [Hu ($n = 4$) or Ma2 ($n = 3$), GAD ($n = 3$), VGKC-complex ($n = 4$) or NMDAR ($n = 3$)] of the patient. Five of the six autopsies were from patients with onconeural antibodies; one was from a patient with VGKC-complex antibody encephalitis who died unexpectedly. Only four of the patients had received immunomodulatory treatments before the specimen was obtained (Table 1).

Magnetic resonance imaging evidence of inflammation or brain atrophy

In one out of six patients with onconeural antibodies, serial MRIs were available. This case with anti-Ma2 limbic encephalitis (Patient

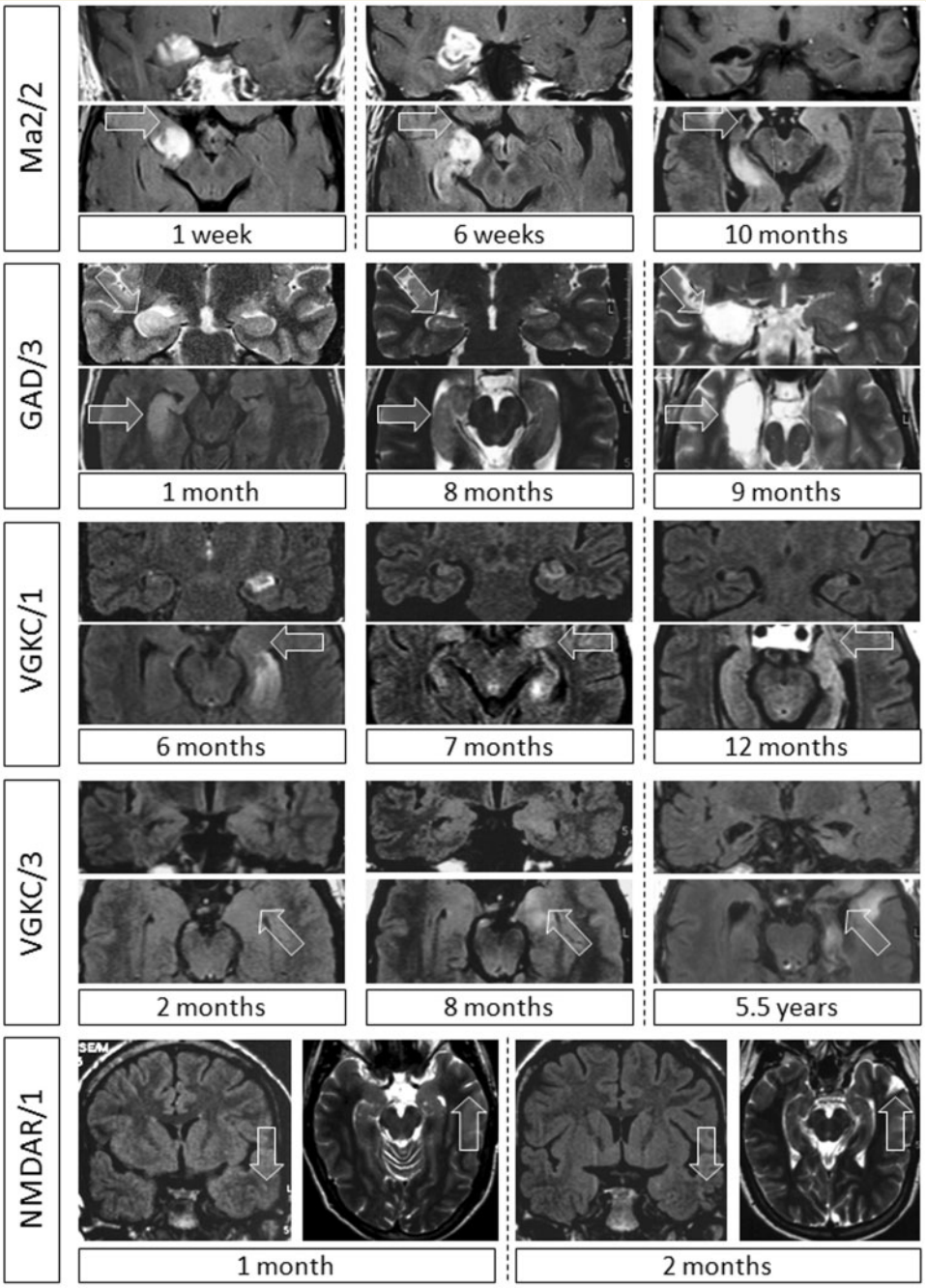

Figure 1 Serial MRI studies of patients associated with antibodies to intracellular or surface antigens. *Top row*: T_1 with contrast enhancement. The remaining images are FLAIR (CSF black) or T_2 weighted (CSF white). The dashed lines indicate when specimens for this study were collected. Arrows show the biopsy sites. The Ma2 antibody$^+$ patient (Patient Ma2/2) at 1 and 6 weeks shows right mediotemporal swelling plus (an exceptional finding in antibody-defined encephalitides) initial contrast enhancement. Ten months after onset, the right mediobasotemporal area becomes severely atrophic. In the GAD antibody$^+$ patient (Patient GAD/3) and the VGKC complex antibodies patients (Patients VCGK/1 and VCGK/3), there is an evolution from hippocampal swelling with T_2/FLAIR signal increase (observed within the first 8 months) to hippocampal atrophy with still increased signal (found beyond a disease duration of 8 months). In contrast to these four examples, the patient with NMDAR antibodies (Patient NMDAR/1) does not undergo atrophy.

Ma2/2) showed progressive atrophy of the T_2/FLAIR-hyperintense mediotemporal lobe (Fig. 1). In two out of three anti-GAD cases with limbic encephalitis, mediotemporal atrophy in the context of T_2/FLAIR hyperintensity developed during the disease course. The third patient had previously had unilateral encephalitic T_2-hypersignal in the left amygdala, but at the time of epilepsy surgery, MRI was normal and without mediotemporal brain atrophy, despite a 10-year disease history. In both patients with VGKC-complex antibodies and serial brain MRIs, brain atrophy developed in areas of encephalitic T_2/FLAIR-hypersignal (Fig. 1).

In contrast, none of the three NMDAR antibody$^+$ patients developed T_2/FLAIR-hypersignal or brain atrophy (Fig. 1).

Neuronal pathology

Neuronal cell loss was seen on MAP2/NeuN stained sections in five out of seven IAg-onconeural cases, two out of three IAg-GAD cases and one out of seven surface antigen (VGKC-complex) cases (Fig. 2A, C, E, H and K). The most severe neuronal loss was found in one anti-Hu, one anti-Ma2, one anti-GAD and one anti-VGKC-complex case. TUNEL reactivity revealed that most cases only had limited (occasional cells) acute neuronal death, but a single autopsy case (Patient VGKC/2), showed numerous TUNEL$^+$ neurons in the CA4 region and dentate gyrus of the hippocampus (Fig. 3H and I). In addition, most of the tissue from those patients showed axonal damage demonstrated by amyloid precursor protein positive spheroids and accumulation of amyloid precursor protein in the cell bodies of neurons (Fig. 2B, D, F, G, I, J and L). In contrast, in all three anti-NMDAR biopsy cases, pathological evidence of neuro-axonal injury was notably absent.

Histochemical staining for Luxol fast blue and immunohistochemistry for 2′,3′-cyclic nucleotide 3′-phosphodiesterase (CNPase) and proteolipid protein did not reveal loss of oligodendrocytes or evidence of demyelination, and staining for glial fibrillary acidic protein did not reveal astrocyte loss, in either group.

Immunopathology

Inflammation

We quantified the numbers of parenchymal T cells, B cells, plasma cells, macrophages and microglial cells. The results are given for the individual patients in Table 2, and summarized in Table 3. Overall, there was a large variation in the absolute numbers of CD3$^+$ T cells (1.2–1188/mm^2) between the individual specimens (Tables 2 and 3). However, in one of the three biopsies from the IAg-GAD patients and all three biopsies of NMDAR antibody$^+$ patients, the density of parenchymal infiltrating CD3$^+$ T cells was low, within the range of neurodegeneration controls, although still higher than that of the healthy controls (Table 2). Density of inflammatory cells in all anti-NMDAR cases was lower than in the other groups, although T cell numbers exceeded those observed in normal controls and were in the range of the neurodegeneration controls (Table 3).

T cell cytotoxicity

In all specimens, CD3$^+$ lymphocytes comprised the majority of parenchyma invading inflammatory cells (Table 3; Figs 3A, D, 4A, D and G). There was a clear difference in the percentage of parenchymal CD8$^+$ T cells (ratio CD8/CD3) between IAg-onconeural (mean 75%, Figs 4B, E, H and 5) and surface antigen (mean 43%, Figs 3B, E and 5) cases ($P < 0.05$). The percentage of CD8 T cells in the IAg-GAD group was intermediate (54%) between the IAg-onconeural and surface antigen groups and not significantly different from both groups. The CD8/CD3 ratio of the surface antigen group also was significantly different from the Rasmussen encephalitis group (Fig. 5, $P < 0.001$). For comparison, we also determined the CD8/CD3 ratio in the perivascular space of blood vessels. Generally in a specific patient the ratio was lower than in the parenchyma (Table 2) confirming that generally CD8 T cells migrate into the parenchyma more readily than CD4 T cells. Unexpectedly, however, the perivascular CD8/CD3 ratio in the NMDAR antibody patients was higher than those in the corresponding parenchyma. These results are based on single immunostainings with CD3 and CD8 on consecutive sections, but were confirmed on sections double-labelled for CD4 and CD8 (Figs 3G and 4I). In addition, we determined the percentage of GrB$^+$/CD3$^+$ cells. There was a high GrB percentage in the IAg-onconeural group compared with the IAg-GAD and surface antigen groups, but no significant difference between the different groups was reached (Fig. 5). In all respects, the IAg-onconeural specimens were very similar to those found in the Rasmussen encephalitis control group in which T cell cytoxicity is well established (Bien *et al*., 2002).

Apposition of multiple GrB$^+$ lymphocytes to single neurons, consistent with a specific cytotoxic T cell attack, was observed in five of seven IAg-onconeural cases (Fig. 4C, F, J–L), and in one of the IAg-GAD cases (Patient GAD/3). The amount of multiple apposition in the IAg-onconeural group was higher than those seen in the surface antigen group in which no multiple appositions were detected (IAg-onconeural versus surface antigen group: $P = 0.02$, two-sided Fisher's exact test, Fig. 3C, F and Table 3). Again, the IAg-onconeural group was similar (no significant difference) to the Rasmussen encephalitis control group in which 6 out of 22 showed such multiple appositions. In the IAg-GAD group one out of three patients also showed such multiple appositions. The IAg-GAD group did not show significant differences with both the IAg-onconeural, the surface antigen group and the Rasmussen encephalitis specimens (Table 3). We also stained sections for CD107a (lysosomal-associated membrane protein-1, lamp-1), a marker that only appears on the cell surface of T lymphocytes after the release of cytotoxic granules (Betts *et al*., 2003). In areas where GrB$^+$ lymphocytes were present, CD107a$^+$ lymphocytes were also detected (Fig. 4M and N). In the IAg-onconeural group, dual staining revealed punctuate reactivity for CD107a overlapping that of GrB within cytotoxic T lymphocytes (Fig. 4P and Q). In addition, CD107a also appeared to be fused with the membranes of some T lymphocytes in a polarized fashion (Fig. 4O), indicating release of cytotoxic granules from cells that were often found in close apposition to neurons. Occasionally, polarized CD107a was a notable finding in the absence of GrB, suggesting that GrB had been released previously (Fig. 4Q and R). These GrB and CD107a findings mirror the stages of a GrB-mediated cytotoxic T cell attack *in vitro* (Hahn *et al*., 1994; Betts *et al*., 2003) and suggest that a cytotoxic T cell mediated immune response is responsible for neuronal cell death in the IAg-onconeural as well as in one of the three cases of the IAg-GAD group. MHC class I expression is a necessary prerequisite for cytotoxic T cell mediated killing. We found expression of MHC class I on neurons in inflammatory sites in all groups (data not shown).

Immunoglobulin and complement deposition

Diffuse cytoplasmic IgG, detected with anti-human IgG, was evident in both neurons and astrocytes in most cases from all groups

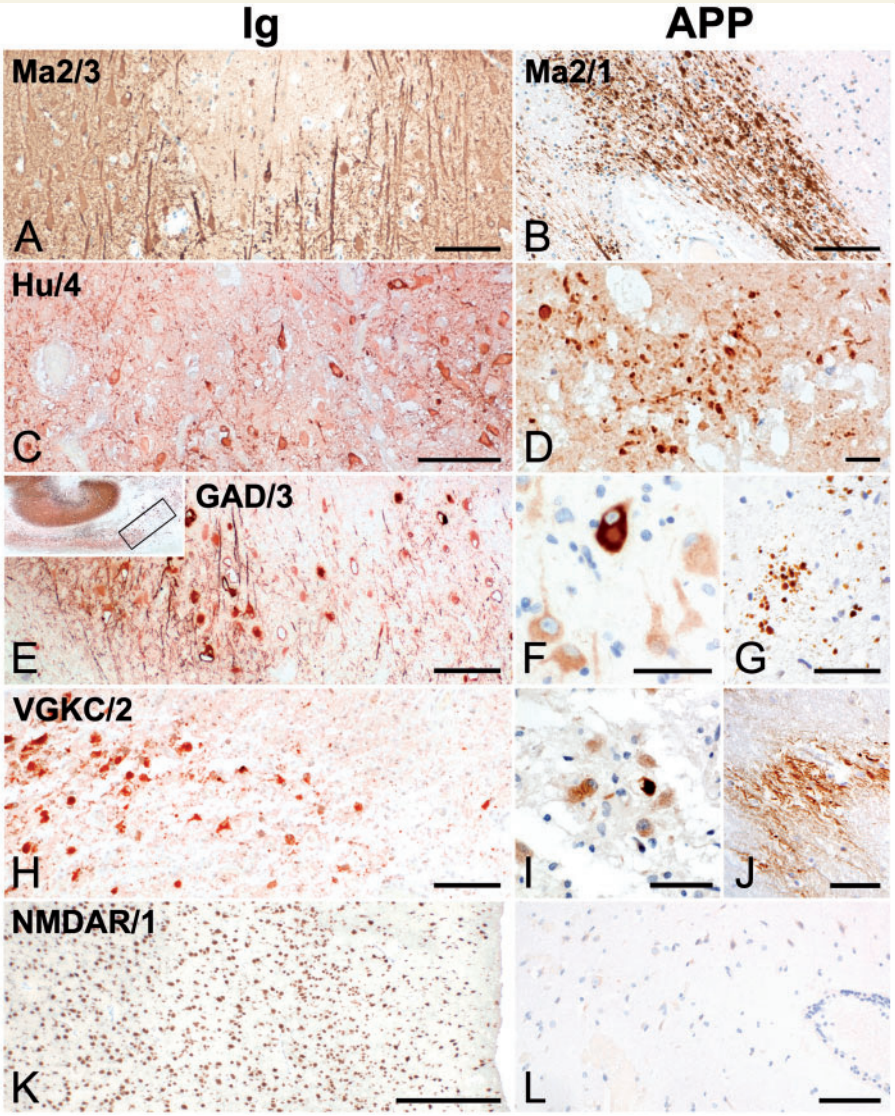

Figure 2 Neuronal pathology of encephalitides defined by antibodies to intracellular or surface antigens. Neuronal pathology in encephalitides associated with antibodies to intracellular antigen and surface antigen. (**A** and **B**) Anti-Ma2 encephalitis in Patients Ma2/3 and Ma2/1. MAP2 staining (**A**) shows neuronal loss in the CA2 region of the hippocampus. Scale bar = 200 μm. In addition, the amyloid precursor protein (APP) staining (**B**) shows a large bundle of degenerating axons. Scale bar = 100 μm. (**C** and **D**) Anti-Hu encephalitis, Patient Hu/4. (**C**) MAP2 staining shows loss of cortical neurons. Scale bar = 100 μm. (**D**) Amyloid precursor protein staining in the same area shows axonal degeneration. Scale bar = 20 μm. (**E–G**) Anti-GAD65 encephalitis, Patient GAD/3. (**E**) MAP2 staining. The *upper* panel shows an overview of the hippocampus. The *insert* shows the CA2/3 transitional area of the hippocampus, which is enlarged in the *lower* panel (scale bar = 200 μm) and reveals clear loss of neurons. (**F**) Amyloid precursor protein staining in the same area shows a darkly stained damaged neuron, indicating loss of axonal transport, in the midst of lightly stained normal amyloid precursor protein positive neurons. Scale bar = 40 μm. (**G**) In addition, the hippocampal alveus shows amyloid precursor protein positive axonal spheroids. Scale bar = 10 μm. (**H–J**) Anti-VGKC encephalitis in Patient VGKC/2 (LGI1 and CASPR2 antibody status unknown) (**H**, scale bar = 100 μm): MAP2 staining shows loss of neurons in the CA2 region of the hippocampus (**I**, scale bar = 40 μm). Amyloid precursor protein staining shows a darkly stained degenerating neuron in the same area (**J**, scale bar = 40 μm). Here amyloid precursor protein shows axonal damage in the alveus of the hippocampus. (**K** and **L**) Anti-NMDAR encephalitis, Patient NMDAR/1. (**K**) NeuN staining of the cortex does not show loss of neurons. Scale bar = 500 μm. (**L**) In addition, the amyloid precursor protein staining shows the absence of axonal damage. Scale bar = 100 μm.

(Fig. 6), but similar anti-IgG staining patterns were also present in Rasmussen encephalitis and neurodegenerative control samples (data not shown). This diffuse cytoplasmic staining is likely to be the result of non-specific uptake of human immunoglobulin due to leakiness of (damaged) neuronal membranes (Barnett *et al.*, 2009). In the spinal cord of a neuromyelitis optica autopsy control, parenchymal staining for immunoglobulin was seen (Fig. 6A). Strikingly, in anti-VGKC-complex encephalitis, but not in the other conditions, there was also evidence of immunoglobulin on the surface of neurons (Fig. 6K). Staining for C9neo, indicative of

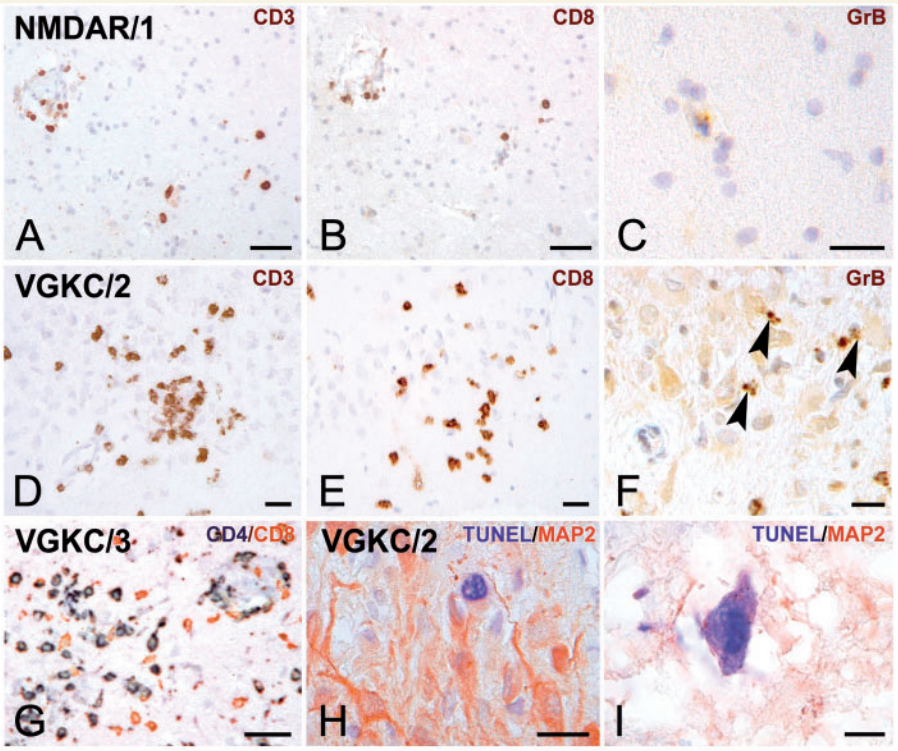

Figure 3 Pathology of brains of encephalitides with antibodies to surface antigens. (**A–C**) Anti-NMDAR encephalitis (Patient NMDAR/1). CD3 (**A**) and CD8 (**B**) staining show infiltration of low numbers of T cells in the parenchyma. Scale bars = 50 μm. Staining for GrB (**C**) shows that part of these T cells contain cytotoxic granules, but such T cells are not seen in apposition to neurons. Scale bar = 20 μm. (**D–J**) Anti-VGKC complex encephalitis (Patient VGKC/2, LGI1 and CASPR2 antibody status unknown). Clearly, in this anti-VGKC case, more $CD3^+$ (**D**) and $CD8^+$ (**E**) cells are present than in the anti-NMDAR encephalitis case. GrB^+ T cells (**F**, arrows) can be found in the vicinity of neurons of the dentate gyrus but multiple appositions are not present. Scale bars: (**D–F**) = 25 μm. (**G**) Patient VGKC/3: double staining for CD4 (blue/black) and CD8 (red) shows that, different from the cases with antibodies to intracellular antigen, in this anti-VGKC case the larger part of T cells are $CD4^+$. Scale bar = 50 μm. (**H** and **I**) Patient VGKC/2: double staining for TUNEL (blue) and MAP2 (red) shows dying neurons in the CA4 region of the hippocampus of an anti-VGKC case in the same area which also shows immunoglobulin and complement C9neo deposition as shown in Fig. 6I and J. Scale bars: (**H**) = 25 μm, (**I**) = 10 μm.

functional activation of the complement cascade, was clearly seen in the parenchyma around blood vessels in the spinal cord of the case with neuromyelitis optica (Fig. 6B), as expected. C9neo was negative in all controls, all cases of the IAg-onconeural and IAg-GAD groups (Fig. 6D, F and H), and all three anti-NMDAR cases (Fig. 6J). However, C9neo deposition was clearly present in the cytoplasm and on the surface of hippocampal CA4 neurons, on neurons in the dentate gyrus and on cortical neurons (Fig. 6L and M) in three out of four anti-VGKC-complex cases. In the case with strongest C9neo deposition (Patient VGKC/2), this deposition co-localized with the TUNEL reactivity seen in $MAP2^+$ neurons (Fig. 3H and I), demonstrating severe acute neuronal death.

Other inflammatory cell types

In addition to cytotoxic T cells, other constituents of the inflammatory infiltrate in these lesions were investigated. There were numerous $CD68^+$ cells (mean density: 229 cells/mm^2) in the brain parenchyma, in part forming microglial nodules (data not shown). The majority of $CD68^+$ cells were microglia; only a mean of 5.3% of the $CD68^+$ cells in the IAg-onconeural group, 0.2% in the IAg-GAD group and 2.1% in the surface antigen group exhibited a macrophage phenotype. $CD20^+$ B cells and $CD138^+$ plasma cells were occasionally found in the meninges and in perivascular cuffs but rarely infiltrated brain parenchyma (Tables 2 and 3). The presence of natural killer and natural killer T cells, which play important roles in immune reactions against tumour cells, was assessed using the marker CD57. Aside from occasional cells in the perivascular space of blood vessels, we did not find any indication of natural killer T cell-mediated killing in the CNS of these patients, confirming earlier studies on natural killer cells in paraneoplastic encephalomyelitis (Jean *et al.*, 1994).

Discussion

There is considerable interest in autoimmune forms of encephalitis associated with specific antibodies to neuronal proteins such as the onconeural antigens, VGKC-complex, NMDAR and GAD. It is generally considered that antibodies to intracellular antigens are good biomarkers for the associated diseases but that the pathology of these conditions is due to T cell cytotoxicity. In contrast, antibodies to the cell surface antigens, VGKC-complex proteins and NMDAR, are thought to be directly pathogenic. However, with the improved recognition and treatment of these patients,

Table 2 Individual data on quantitative immunopathology of patients and control groups

Patient numbers	Number of specimens evaluated	CD3 (cells/mm^2)	CD8 (cells/mm^2)	CD8 (% of CD3 parenchymal)	CD8 (% of CD3 perivascular)	GrB (cells/mm^2)	GrB (% of CD3)	GrB multiple appositions	CD20 (cells/mm^2)	CD138 (cells/mm^2)	Mac (cells/mm^2)	Mic (cells/mm^2)	Complement activation
Patients with antibodies to intracellular antigens													
Ma2/1	3	346.0	228.0	66	32	52.0	15	Yes	6.4	1.3	27.1	304.8	No
Ma2/2	2	1188.0	806.4	68	np	616.7	52	Yes	264.0	224.0	76.0	260.0	No
Ma2/3	1	90.4	81.3	90	65	19.8	22	No	0.0	1.0	0.0	55.5	No
Hu1	1	273.0	205.0	75	52	95.0	35	Yes	126.0	15.0	7.0	369.0	No
Hu2	1	12.3	7.8	63	37	4.0	33	No	0.0	1.4	3.0	60.0	No
Hu3	1	27.8	17.6	64	39	2.9	10	Yes	0.3	1.6	0.0	41.0	No
Hu4	1	396.0	384.0	97	67	132.0	33	Yes	0.4	1.0	0.0	398.0	No
Patients with GAD antibodies													
GAD1	1	2.1	1.3	61	56	0.0	0	No	0.0	0.0	0.3	134.4	No
GAD2	1	7.5	3.9	52	49	0.0	0	No	0.1	0.0	0.6	212.8	No
GAD3	1	70.0	35.0	50	50	1.5	2	Yes	6.5	9.5	0.0	312.0	No
Patients with antibodies to surface antigens													
VGKC1 (LGI1 Abs)	1	5.9	3.1	53	np	0.0	0	No	0.0	0.0	0.0	147.2	Yes
VGKC2 (Ab specificity unknown)	1	13.2	7.0	53	41	4.0	31	No	0.2	0.0	0.6	98.0	Yes
VGKC3 (LGI1/CASPR2 Ab-negative)	1	651.6	324.4	50	28	67.2	10	No	24.0	12.8	18.0	250.0	Yes
VGKC4 (Ab specificity unknown)	1	21.9	9.7	44	np	0.5	2	No	0.0	0.0	0.8	166.0	No
NMDAR1	1	2.8	0.6	23	63	0.0	0	No	2.1	0.8	2.9	129.6	No
NMDAR2	1	1.2	0.4	30	66	0.1	7	No	0.0	0.1	2.5	65.7	No
NMDAR3	1	2.1	0.9	44	56	0.0	0	No	0.0	0.0	2.1	222.4	No
Controls: means (ranges)													
Rasmussen encephalitis	22	19.5 (0.6–127.8)	16.1 (0.4–101.5)	81 (40–100)	ND	7.0 (0.0–42.3)	32(0–94)	6/22 Yes	0.1 (0.0–0.5)	0.1 (0.0–1.6)	0.5 (0.0–5.3)	87.5 (4.0–283.3)	0/22 Yes
Neurodegeneration	25	1.9 (0.2–4.7)	1.2 (0.0–6.5)	58 (0–200[a])	ND	0.2 (0.0–1.0)	14 (0–67)	0/25 Yes	0.0 (0.0–0.0)	0.0 (0.0–0.0)	0.2 (0.0–2.0)	100.0 (30.0–313.0)	0/25 Yes
Normal controls	7	0.1 (0.0–0.3)	0.1 (0.0–0.1)	17 (0–50)	ND	0.0 (0.0–0.1)	15 (0–36)	0/7 Yes	0.0 (0.0–0.0)	0.0 (0.0–0.0)	0.0 (0.0–0.0)	43.6 (20.0–66.0)	0/7 Yes

Multiple appositions relate to neurons engulfed by more than one GrB$^+$ T cell.

a Due to tyramine enhancement, in some samples a 20% increase in CD8$^+$ cells was achieved. This enhanced sensitivity for CD8 together with small individual cell counts in the controls is reflected in occasional '>100%' CD8/CD3 ratios.

GrB = granzyme B; Mac = macrophages; Mic = microglial cells; np = not enough cells in blood vessels present to analyse; ND = not done.

Table 3 Immune cells in encephalitis with antibodies to intracellular and surface antigens

	IAg-onconeural ($n = 7$)	IAg-GAD ($n = 3$)	Surface antigen ($n = 7$)	RE ($n = 22$)	Neurodegeneration ($n = 25$)	Normal controls ($n = 7$)
Demographic data						
Age at specimen collection (years)	52 ± 17	27 ± 31	40 ± 19	16 ± 12	47 ± 26	59 ± 10
Disease duration at specimen collection (months)	6 ± 4	83 ± 54	9 ± 6	53 ± 33	129 ± 190 (without Alzheimer cases)	n.a.
Inflammation						
CD3 (cells/mm^2)	333 ± 377	27 ± 31	100 ± 225	20 ± 29	1.9 ± 1.6	0.1 ± 0.1
CD8	247 ± 259	13 ± 15	49 ± 112	16 ± 23	1.2 ± 1.5	0.1 ± 0
GrB	132 ± 203	0.5 ± 0.7	10 ± 23	7 ± 11	0.2 ± 0.3	0 ± 0
Cases with multiple appositions of GrB$^+$ T cells to neurons	5/7[a]	1/3	0/7	6/22	0/25	0/7
CD20, B cells	57 ± 95	2 ± 3	4 ± 8	0.1 ± 0.2	0 ± 0	0 ± 0
CD138, plasma cells	35 ± 77	12 ± 17	2 ± 4	0.1 ± 0.3	0 ± 0	0 ± 0
CD68, macrophages	16 ± 26	0 ± 0	4 ± 6	0.5 ± 1.3	0.2 ± 0.5	0 ± 0
CD68, microglial cells	213 ± 145	220 ± 73	154 ±60	88 ± 72	100 ± 51	44 ± 17

Cell densities are given as per mm^2 in 4 μm paraffin sections (means ± SD).
a Significantly different from the surface antigen group (test was only performed for comparison of IAg-onconeural, IAg-GAD, surface antigen and Rasmussen encephalitis groups).
n.a. = not applicable; RE = Rasmussen encephalitis.

biopsy and autopsy tissues are seldom available and the immunopathology of the conditions is not well studied. The few reports available have identified 'T cell infiltrates' and most did not attempt to define different T and B cell mediated mechanisms.

The clinical presentations of the disorders studied here are remarkably similar, usually consisting of a combination of neuropsychological impairment and seizures. On the other hand, the newly described encephalitides with antibodies to the VGKC-complex and NMDAR (i.e. surface antigens) have a much better clinical prognosis (Thieben *et al*., 2004; Vincent *et al*., 2004; Dalmau *et al*., 2008; Irani *et al*., 2010*b*) than the classical paraneoplastic encephalitides associated with antibodies to intracellular antigens (Dalmau and Rosenfeld, 2008). This is particularly true in patients with VGKC-complex antibodies, and also in anti-NMDAR encephalitis in which removal of an underlying malignancy (usually ovarian teratoma) can be associated with excellent recovery; clinical outcomes in the patients without detectable tumours are less complete and some relapse (Irani *et al*., 2010*a*; Dalmau *et al*., 2011). These observations have resulted in a conceptual shift from a clinicomorphological (limbic encephalitis), or paraneoplastic versus non-paraneoplastic approach, to an antibody-focused viewpoint with a particular emphasis on the distinction between antibodies to intracellular antigens versus surface antigens (Buckley and Vincent, 2005; Tüzün and Dalmau, 2007; Dalmau and Rosenfeld, 2008; Vincent *et al*., 2010).

Here we tested the hypothesis that encephalitides with intracellular antigens differ in their immune reaction from encephalitides with surface antigens, and that T cells would only play a cytotoxic role in the former group. In the IAg-onconeural group and the IAg-GAD group (non-paraneoplastic GAD cases) we found no evidence of IgG or complement deposition, but we found multiple appositions of GrB$^+$ cytotoxic T cells to neurons, very similar to those previously described in patients with Rasmussen encephalitis (Bien *et al*., 2002; Bauer *et al*., 2007). Moreover, we found that the patients from the IAg-onconeural group had a higher CD8/CD3 ratio than patients with antibodies to surface antigens.

Previous studies in paraneoplastic encephalitis with onconeural antibodies suggested that neuronal damage is induced by a cytotoxic T cell mediated response, demonstrating the presence of T cell intracytoplasmic antigen-1-positive lymphocytes in the vicinity of neurons (Blumenthal *et al*., 2006). Here, we confirmed these observations and provide further evidence for GrB-mediated neuronal cytotoxicity showing both release of GrB and detection of CD107a on the surface of T cells. These findings mirror the stages of GrB-mediated cytotoxic T cell attack documented *in vitro* (Hahn *et al*., 1994; Betts *et al*., 2003).

The results of the IAg-GAD cases, however, were somewhat different from the paraneoplastic cases with intracellular antigen antibodies. Although not significant, the CD8/CD3 ratio in the GAD antibody$^+$ cases was lower than those of the paraneoplastic cases, and within the range of the highest ratios of the surface antigen group. In addition, one of the three anti-GAD cases (Patient GAD/1) showed T cell numbers that were as low as those of the anti-NMDAR cases. This particular patient, however, did not develop atrophy on MRI, compatible with the hypothesis that T cells are relevant to, or perhaps requisite for, neuronal loss and the development of atrophy in patients with GAD antibodies. It remains a question why the T cell numbers and the CD8/CD3 ratio in these GAD patients are rather low compared to the other cases with antibodies against intracellular antigens. The absence of an underlying malignancy may be a reason, but also the long disease duration time in two patients may bias this result towards less intense inflammation. The syndrome of epilepsy and limbic encephalitis with GAD antibodies has only recently been studied

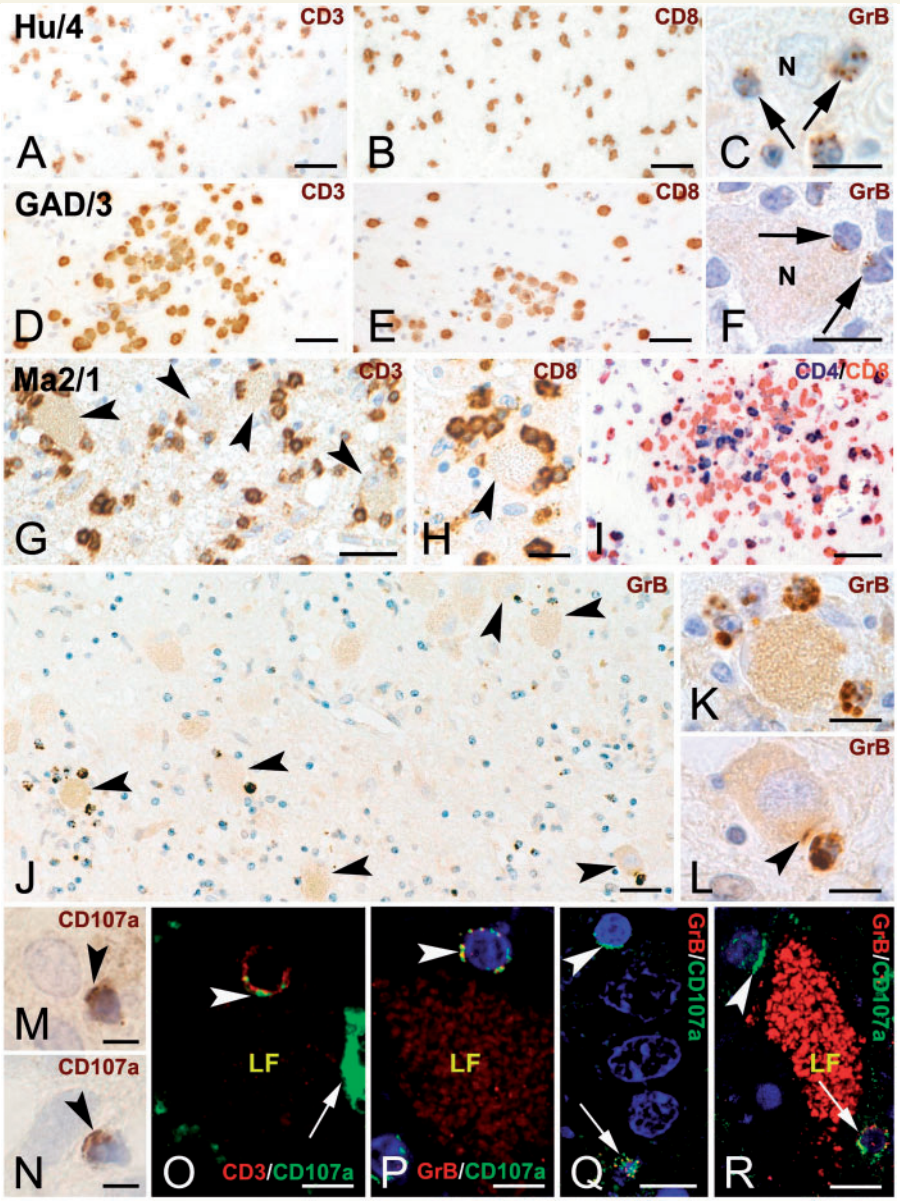

Figure 4 Pathology of brains of encephalitides with antibodies to intracellular antigens. (**A–C**) Anti-Hu (paraneoplastic) encephalitis (Patient Hu/4). Staining for CD3 (**A**) and CD8 (**B**) show prominent perivascular and parenchymal infiltration of T cells. (**C**) Staining for GrB (arrows) shows multiple appositions of these cells to a neuron. Scale bars: **A**, **B** = 100 μm, **C** = 20 μm. (**D–F**) Anti-GAD encephalitis (Patient GAD/3). Multiple $CD3^+$ cells (**D**) and $CD8^+$ cells (**E**) are seen in the parenchyma. (**F**) Staining for GrB in this GAD case shows apposition of two cytotoxic T cells with polarized granules towards a neuron. Scale bars: (**D** and **E**) = 100 μm, (**F**) = 20 μm. (**G–R**) Anti-Ma-2 antibody (paraneoplastic) encephalitis (Patient Ma2/1). (**G**) Multiple neurons (arrowheads) are surrounded by multiple $CD3^+$ T lymphocytes. (**H**) Staining for CD8 in the same area shows that these encircling T cells are also $CD8^+$. Scale bars: (**G** and **H**) = 50 μm. (**I**) Double staining for CD4 (blue) and CD8 (red) shows that the larger part of T cells are $CD8^+$. Scale bar: (**I**) = 50 μm. (**J**) Staining for GrB in the same area as (**G**) and (**H**) shows that several neurons (arrows) have multiple appositions of GrB^+ cytototxic T cells attached to them (same area as **G** and **H**). (**K**) Higher magnification of a neuron with multiple attached GrB^+ T lymphocytes. Scale bar = 10 μm. (**L**) Another GrB^+ T lymphocyte in close apposition to a neuron. In this case, GrB reactivity is seen on the neuronal membrane (arrowhead) indicating release of GrB from the T cell. Scale bar = 10 μm. (**M** and **N**) Two examples of lymphocytes attached to neurons. A polarized membranous CD107a staining is seen, indicating release of cytotoxic granules. Scale bars = 5 μm. (**O**) Confocal double staining for CD3 (red) and CD107a (green) shows a lymphocyte in apposition to a neuron [indicated by lipofuscin (LF)]. The signal for CD107a (arrowhead) overlaps with the staining for CD3 indicating fusion of cytotoxic granules with the membrane during release. The arrow shows CD107a in perineuronal microglia. In (**P**), a lymphocyte with GrB^+ (red) granules in a non-polarized localization in apposition to a neuron (LF) is shown. The GrB signal overlaps with the signal for CD107a, indicating that no release of GrB has taken place. Scale bar = 5 μm. (**Q** and **R**) Two examples of confocal double staining for GrB (red) and CD107a (green). (**Q**) A lymphocyte in which CD107a is colocalized with GrB (arrow). A second lymphocyte lies in apposition to a neuron and shows polarized membranous-like CD107a in the absence of GrB (arrowhead) indicating previous release of the cytotoxic compound. Scale bar = 10 μm. The same can be seen in (**R**). Again a $CD107a^+/GrB^+$ T lymphocyte without polarization and a $CD107a^+/GrB^-$ T lymphocyte (arrowhead) with polarization is shown in close apposition to a neuron. Scale bar = 10 μm.

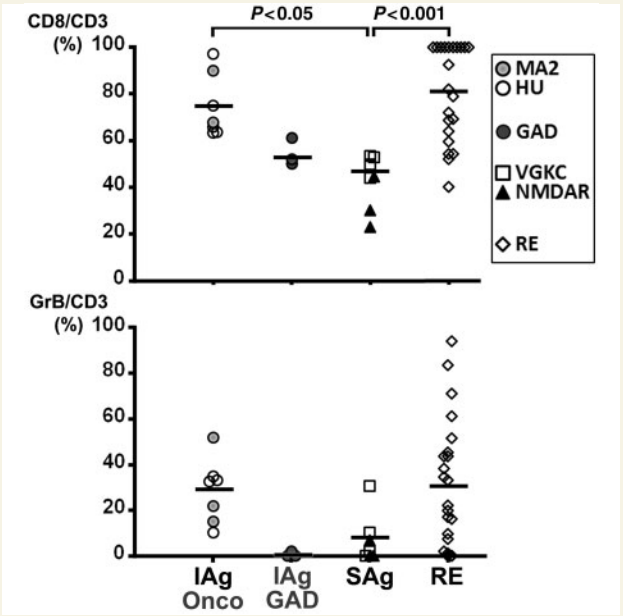

Figure 5 CD8/CD3 and GrB/CD3 ratios in patients with antibodies to intracellular or surface antigens and compared to Rasmussen encephalitis (RE).

(Malter *et al*., 2010) and this is, we believe, the first description of the pathology in a series of cases. Besides the presence of multiple cytotoxic T cells in close apposition to target neurons, our stainings showed severe neuronal loss and axonal dystrophy in the hippocampus in two out of three patients. Importantly, immunoglobulin and complement deposition was completely absent. In general, the pathogenic role of GAD antibodies is not clear because of the different clinical syndromes with which they are associated (stiff person syndrome, cerebellar ataxia and limbic encephalitis). Since the antigen is intracellular, a T cell-mediated pathology would be a likely mechanism. Interestingly, in peripheral diseases such as juvenile diabetes, anti-GAD antibodies as well as T cell cytotoxicity against GAD65 are present (Panina-Bordignon *et al*., 1995; Viglietta *et al*., 2002). On the other hand, however, GAD antibodies are seldom associated with malignancies and the beneficial effects of immunotherapies, including intravenous immunoglobulins, have been demonstrated in case reports and in a randomized clinical trial (Dalakas *et al*., 2001) suggesting similarities with diseases associated with surface antigens, albeit with lesser treatment responses (Malter *et al*., 2010). The more frequent occurrence of unmatched oligoclonal bands in patients with GAD antibodies brings them closer to the surface antigen patients than to the IAg-onconeural patients (Table 1). One explanation for these observations could be the existence of pathogenic surface antigen antibodies coexisting with GAD antibodies (Vincent *et al*., 1999); indeed, co-existence of GAD and GABA-B receptor antibodies has been reported in a small number of patients with limbic encephalitis (Lancaster *et al*., 2010; Boronat *et al*., 2011). Also, in stiff person syndrome with GAD antibodies, additional cell-surface antibodies have been observed (Chang and Vincent, in preparation). Such an additional surface antigen antibody might be an alternative explanation for the relatively low CD8/CD3 and GrB/CD3 ratios in our IAg-GAD patients. Thus, although our findings support the hypothesis that encephalitides with intracellular antigen antibodies are mediated by cytotoxic T cells, this hypothesis may be too restricted since it does not take into account the possibility that multiple antibodies against both intracellular antigens, as well as surface antigens, exist in patients with GAD antibodies.

The second group that we investigated was the group with surface antigen antibodies. Intriguingly these two surface antigen antibody diseases differ strongly in terms of immunopathology. The neocortex of NMDAR antibody-positive patients showed almost no inflammation, and no clear signs of neuronal loss. By contrast, there was loss of neurons with evidence of IgG and complement deposition in the VGKC-complex antibody-positive cases. The distinction between cases with or without neuronal loss was reflected by MRI features, with atrophy restricted to patients with VGKC-complex antibodies. Consistent with our findings, Tüzün *et al*. (2009) found only rare infiltrating inflammatory cells and absence of complement in the brains of patients with anti-NMDAR encephalitis and hippocampal neuronal loss was detected in only one of four brains studied by Dalmau *et al.* (2008). Concordantly, follow-up MRI studies in many patients show absence of brain atrophy. Existing non-quantitative neuropathological evidence in anti-NMDAR encephalitis shows hippocampal pyramidal cell loss but only mild inflammation (Tüzün *et al*., 2009; Camdessanche *et al*., 2011). In our anti-NMDAR cases with neocortical samples only, we did not observe clear cell loss, signs of acute cell damage or atrophy on brain MRI. Furthermore there were few infiltrating T cells, their numbers were lower than in the other antibody-defined subgroups and in the range of neurodegenerative controls. In contrast to VGKC-complex antibody-positive cases, we found no evidence of complement activation, consistent with previous case reports (Tüzün *et al*., 2009; Hughes *et al*., 2010). Experimental evidence suggests that the NMDAR antibodies act by reducing the density of NMDAR clusters by cross-linking and subsequent internalization of the receptors, leading to a state of reversible NMDAR hypofunction (Hughes *et al*., 2010). Taken together, even though NMDAR antibodies appear to be involved in the clinical disease process, there is no evidence in favour of classical cytotoxic T cell-mediated or antibody and complement-mediated neuronal cell death in our cases. The possibility that a more active inflammatory infiltrate or antibody deposition could be found at an earlier disease stage in both the hippocampus and cortex, cannot be excluded, although it is striking that MRI evidence of inflammation in the hippocampus is rare in this condition. An exclusive effect of the antibodies in reducing NMDAR expression in the hippocampus, however, would be difficult to reconcile with the complex progression of the disease that begins with features which could stem from medial temporal lobe dysfunction but progresses to a much broader clinical phenotype (Dalmau *et al*., 2008; Irani *et al*., 2010*b*).

In the three previous VGKC-complex antibody autopsy case studies, which lacked the detail provided here, scattered T cell infiltration (Dunstan and Winer, 2006; Park *et al*., 2007) perivascular B cell accumulation and an intraparenchymal infiltrate with predominance of $CD4^+$ T cells have been reported (Khan *et al*.,

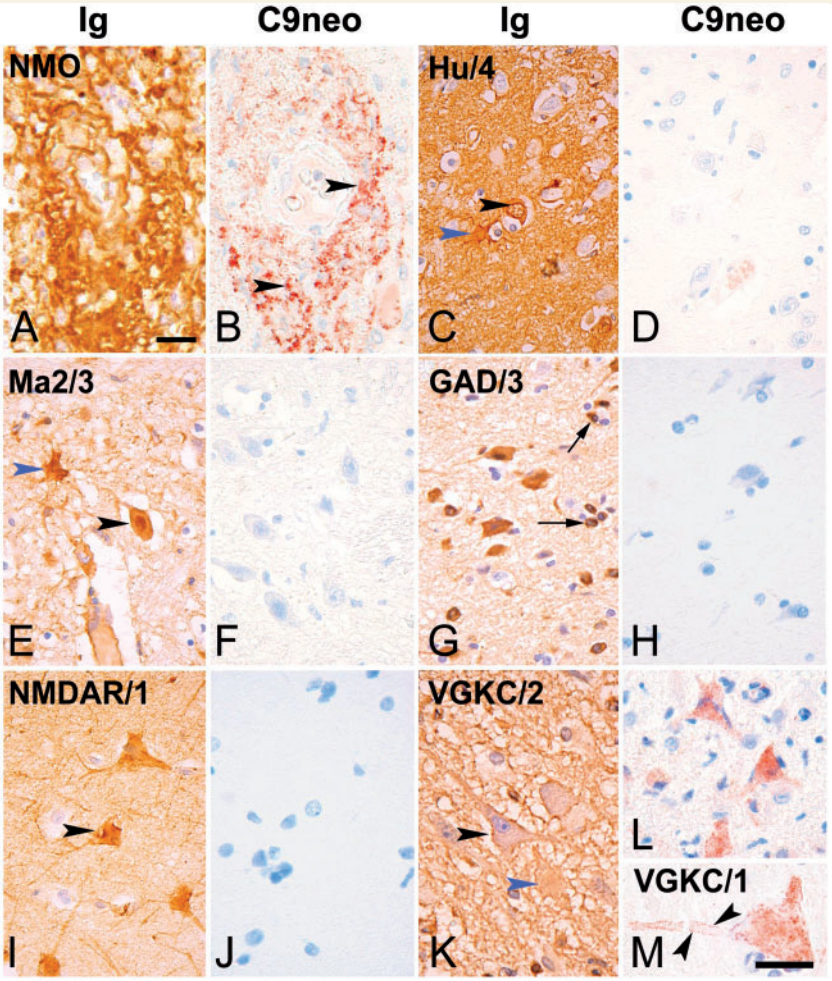

Figure 6 Immunoglobulin and complement in patients with antibodies to intracellular and surface antigens. Staining for immunoglobulin G (**A**, **C**, **E**, **G**, **I** and **K**) and complement C9 (C9, **B**, **D**, **F**, **H**, **J**, **L** and **M**) in comparable areas in the intracellular antigen group and surface antigen group. (**A** and **B**) Immunoglobulin staining (**A**) and C9neo deposition (arrowheads in **B**) in the spinal cord of a positive control patient with neuromyelitis optica (NMO). (**C** and **D**) Ig and C9 neo in a patient with paraneoplastic encephalomyelitis with Hu antibodies (Patient Hu/4), a patient with Ma-2 antibodies (**E** and **F**, Patient Ma2/1), in non-paraneoplastic encephalitis with GAD65 antibodies (**G** and **H**, Patient GAD/3), NMDAR antibodies (**I** and **J**, Patient NMDAR/1) or VGKC antibodies (**K–M**, Patient VGKC/2). IgG stainings show uptake of IgG in neurons in anti-Hu (**C**), anti-Ma-2 (**E**), anti-GAD (**G**) and anti-NMDAR cases (**I**). In addition, in most cases astrocytes also reveal cytoplasmic staining for IgG (blue arrowheads in **C**, **E** and **K**). In contrast, in the VGKC case (**K**), staining for Ig is seen on the surface of neurons. Complement C9 staining was negative in all cases except for three out of four anti-VGKC cases where a punctuate staining (**L**) of neurons in the CA4 area of the hippocampus can be seen. A second VGKC case revealed a punctate staining as well as surface staining (arrowheads) of single cortical neurons (**M**). Scale bar: (**A–L**) = 20 μm, (**M**) = 10 μm.

2009). We found variably intense inflammation and overall a lower CD8/CD3 ratio than in the patients with antibodies to intracellular antigens. Although GrB^+ T cells were present in the lesions we did not observe apposition of these cells to neurons or release of GrB, therefore T cell cytotoxicity in our view is not a major contributor. However, immunoglobulin and complement deposition on neurons was a prominent finding and TUNEL reaction in the same area demonstrated acute neuronal cell death. This suggests antibody and complement mediated neuronal cell damage in patients with VGKC-complex antibodies. This is interesting since IgG4 rather than complement-activating IgG1 antibodies dominate in sera of patients with VGKC-complex antibody encephalitis (unpublished data). Recent findings show that the antibodies that immunoprecipitate dendrotoxin-labelled VGKC-complexes are in fact directed to LGI1 or CASPR2 or other undefined components of the VGKC-complex (Irani *et al*., 2010*a*; Lai *et al*., 2010). One of our three cases with C9neo deposition was LGI1 antibody-positive, the second case was negative for both LGI1 and CASPR2, and in the third case (with extensive C9neo deposition on neural somata and neuronal death), serum for LGI1/CASPR2 retesting unfortunately was not available. Although LGI1 is the predominant target in VGKC-complex antibody-positive limbic encephalitis, some patients have CASPR2 antibodies (Irani *et al*., 2010*a*).

There are several limitations of our study: (i) disease duration at specimen collection was always >1 month and reached a mean value of 21 months. This indicates that our results describe the

immune-reaction in the chronic rather than the acute disease stage; (ii) in the patients with limited sampling (epilepsy surgery, brain biopsies), sampling errors may have occurred and (iii) a proportion of the patients had received prior immunosuppressive treatment (details in Table 1), potentially reducing or changing the immunopathological appearance. Yet, the overall consistency of the results suggests that these potential confounders did not exert a major effect.

Despite the limitations that are intrinsic to the study of human material, our work suggests clear immunopathological differences, related to the hypothesized intracellular antigen and surface antigen groups, but even more so between subgroups defined by the nature of the antibodies. Elevated CD8/CD3 ratios in diseases associated with antibodies to intracellular antigens, suggests a cytotoxic T cell-driven pathomechanism. In diseases with antibodies to surface antigens, our findings support a B cell/plasma cell-related pathomechanism, with evidence of a complement-mediated pathogenesis in patients with VGKC-complex antibodies. This immunopathogenic dichotomy parallels other neurological autoimmune disorders such as polymyositis and dermatomyositis, which have a predominant T cell and humorally mediated pathogenesis, respectively (Arahata and Engel, 1984). These observations may contribute to a rational choice in immunological treatments for these disorders.

Acknowledgements

We would like to thank Marianne Leisser, Angela Kury, Ulrike Köck und Claudia Ullmann for expert technical help. We also like to thank Prof. Dr Jeanne Bell (Pathology Directorate, Royal Infirmary Edinburgh, UK) for providing us with patient material and Prof. Dr Horst Urbach, University of Bonn, Department of Radiology/Neuroradiology for providing and discussing magnetic resonance images.

Supplementary material

Supplementary material is available at *Brain* online.

References

Arahata K, Engel AG. Monoclonal antibody analysis of mononuclear cells in myopathies. I: Quantitation of subsets according to diagnosis and sites of accumulation and demonstration and counts of muscle fibers invaded by T cells. Ann Neurol 1984; 16: 193–208.

Barnett M, Prosser J, Sutton I, Halmagyi GM, Davies L, Harper C, et al. Paraneoplastic brain stem encephalitis in a woman with anti-Ma2 antibody. J Neurol Neurosurg Psychiatry 2001; 70: 222–5.

Barnett MH, Parratt JD, Cho ES, Prineas JW. Immunoglobulins and complement in postmortem multiple sclerosis tissue. Ann Neurol 2009; 65: 32–46.

Bauer J, Elger CE, Hans VH, Schramm J, Urbach H, Lassmann H, et al. Astrocytes are a specific immunological target in Rasmussen's encephalitis. Ann Neurol 2007; 62: 67–80.

Bernal F, Graus F, Pifarre A, Saiz A, Benyahia B, Ribalta T. Immunohistochemical analysis of anti-Hu-associated paraneoplastic encephalomyelitis. Acta Neuropathol 2002; 103: 509–15.

Betts MR, Brenchley JM, Price DA, De Rosa SC, Douek DC, Roederer M, et al. Sensitive and viable identification of antigen-specific $CD8^+$ T cells by a flow cytometric assay for degranulation. J Immunol Methods 2003; 281: 65–78.

Bien CG, Bauer J, Deckwerth TL, Wiendl H, Deckert M, Wiestler OD, et al. Destruction of neurons by cytotoxic T cells: a new pathogenic mechanism in Rasmussen's encephalitis. Ann Neurol 2002; 51: 311–8.

Bien CG, Urbach H, Schramm J, Soeder BM, Becker AJ, Voltz R, et al. Limbic encephalitis as a precipitating event in adult-onset temporal lobe epilepsy. Neurology 2007; 69: 1236–44.

Blumenthal DT, Salzman KL, Digre KB, Jensen RL, Dunson WA, Dalmau J. Early pathologic findings and long-term improvement in anti-Ma2-associated encephalitis. Neurology 2006; 67: 146–9.

Boronat A, Sabater L, Saiz A, Dalmau J, Graus F. GABA(B) receptor antibodies in limbic encephalitis and anti-GAD-associated neurologic disorders. Neurology 2011; 76: 795–800.

Buckley C, Vincent A. Autoimmune channelopathies. Nat Clin Pract Neurol 2005; 1: 22–33.

Camdessanche JP, Streichenberger N, Cavillon G, Rogemond V, Jousserand G, Honnorat J, et al. Brain immunohistopathological study in a patient with anti-NMDAR encephalitis. Eur J Neurol 2011; 18: 929–31.

Dalakas MC, Fujii M, Li M, Lutfi B, Kyhos J, McElroy B. High-dose intravenous immune globulin for stiff-person syndrome. N Engl J Med 2001; 345: 1870–6.

Dalmau J, Gleichman AJ, Hughes EG, Rossi JE, Peng X, Lai M, et al. Anti-NMDA-receptor encephalitis: case series and analysis of the effects of antibodies. Lancet Neurol 2008; 7: 1091–8.

Dalmau J, Lancaster E, Martinez-Hernandez E, Rosenfeld MR, Balice-Gordon R. Clinical experience and laboratory investigations in patients with anti-NMDAR encephalitis. Lancet Neurol 2011; 10: 63–74.

Dalmau J, Rosenfeld MR. Paraneoplastic syndromes of the CNS. Lancet Neurol 2008; 7: 327–40.

Dunstan EJ, Winer JB. Autoimmune limbic encephalitis causing fits, rapidly progressive confusion and hyponatraemia. Age Ageing 2006; 35: 536–7.

Graus F, Keime-Guibert F, Rene R, Benyahia B, Ribalta T, Ascaso C, et al. Anti-Hu-associated paraneoplastic encephalomyelitis: analysis of 200 patients. Brain 2001; 124 (Pt 6): 1138–48.

Graus F, Saiz A, Dalmau J. Antibodies and neuronal autoimmune disorders of the CNS. J Neurol 2010; 257: 509–17.

Hahn K, DeBiasio R, Tishon A, Lewicki H, Gairin JE, LaRocca G, et al. Antigen presentation and cytotoxic T lymphocyte killing studied in individual, living cells. Virology 1994; 201: 330–40.

Hughes EG, Peng X, Gleichman AJ, Lai M, Zhou L, Tsou R, et al. Cellular and synaptic mechanisms of anti-NMDA receptor encephalitis. J Neurosci 2010; 30: 5866–75.

Iizuka T, Yoshii S, Kan S, Hamada J, Dalmau J, Sakai F, et al. Reversible brain atrophy in anti-NMDA receptor encephalitis: a long-term observational study. J Neurol 2010; 257: 1686–91.

Irani SR, Alexander S, Waters P, Kleopa KA, Pettingill P, Zuliani L, et al. Antibodies to Kv1 potassium channel-complex proteins leucine-rich, glioma inactivated 1 protein and contactin-associated protein-2 in limbic encephalitis, Morvan's syndrome and acquired neuromyotonia. Brain 2010a; 133: 2734–2748.

Irani SR, Bera K, Waters P, Zuliani L, Maxwell S, Zandi MS, et al. N-methyl-D-aspartate antibody encephalitis: temporal progression of clinical and paraclinical observations in a predominantly non-paraneoplastic disorder of both sexes. Brain 2010b; 133: 1655–67.

Jean WC, Dalmau J, Ho A, Posner JB. Analysis of the IgG subclass distribution and inflammatory infiltrates in patients with anti-Hu-associated paraneoplastic encephalomyelitis. Neurology 1994; 44: 140–7.

Khan NL, Jeffree MA, Good C, Macleod W, Al-Sarraj S. Histopathology of VGKC antibody-associated limbic encephalitis. Neurology 2009; 72: 1703–5.

Lai M, Hughes EG, Peng X, Zhou L, Gleichman AJ, Shu H, et al. AMPA receptor antibodies in limbic encephalitis alter synaptic receptor location. Ann Neurol 2009; 65: 424–34.

Lai M, Huijbers MG, Lancaster E, Graus F, Bataller L, Balice-Gordon R, et al. Investigation of LGI1 as the antigen in limbic encephalitis previously attributed to potassium channels: a case series. Lancet Neurol 2010; 9: 776–85.

Lancaster E, Lai M, Peng X, Hughes E, Constantinescu R, Raizer J, et al. Antibodies to the GABA(B) receptor in limbic encephalitis with seizures: case series and characterisation of the antigen. Lancet Neurol 2010; 9: 67–76.

Lancaster E, Martinez-Hernandez E, Titulaer MJ, Boulos M, Weaver S, Antoine JC, et al. Antibodies to metabotropic glutamate receptor 5 in the Ophelia syndrome. Neurology 2011; 77: 1698–701.

Malter MP, Helmstaedter C, Urbach H, Vincent A, Bien CG. Antibodies to glutamic acid decarboxylase define a form of limbic encephalitis. Ann Neurol 2010; 67: 470–8.

Niehusmann P, Dalmau J, Rudlowski C, Vincent A, Elger CE, Rossi JE, et al. Diagnostic value of N-methyl-D-aspartate receptor antibodies in women with new-onset epilepsy. Arch Neurol 2009; 66: 458–64.

Panina-Bordignon P, Lang R, van Endert PM, Benazzi E, Felix AM, Pastore RM, et al. Cytotoxic T cells specific for glutamic acid decarboxylase in autoimmune diabetes. J Exp Med 1995; 181: 1923–7.

Park DC, Murman DL, Perry KD, Bruch LA. An autopsy case of limbic encephalitis with voltage-gated potassium channel antibodies. Eur J Neurol 2007; 14: e5–6.

Piccolo G, Tavazzi E, Cavallaro T, Romani A, Scelsi R, Martino G. Clinico-pathological findings in a patient with progressive cerebellar ataxia, autoimmune polyendocrine syndrome, hepatocellular carcinoma and anti-GAD autoantibodies. J Neurol Sci 2010; 290: 148–9.

Saiz A, Dalmau J, Butler MH, Chen Q, Delattre JY, De Camilli P, et al. Anti-amphiphysin I antibodies in patients with paraneoplastic neurological disorders associated with small cell lung carcinoma. J Neurol Neurosurg Psychiatry 1999; 66: 214–7.

Schwab N, Bien CG, Waschbisch A, Becker A, Vince GH, Dornmair K, et al. $CD8^+$ T cell clones dominate brain infiltrates in Rasmussen encephalitis and persist in the periphery. Brain 2009; 132: 1236–46.

Soeder BM, Urbach H, Elger CE, Bien CG, Beyenburg S. VGKC-Antikörper-assoziierte limbische Enzephalitis [Limbic encephalitis associated with autoantibodies against voltage-gated potassium channels.]. Nervenarzt 2005; 76: 760–2.

Stam NJ, Vroom TM, Peters PJ, Pastoors EB, Ploegh HL. HLA-A- and HLA-B-specific monoclonal antibodies reactive with free heavy chains in western blots, in formalin-fixed, paraffin-embedded tissue sections and in cryo-immuno-electron microscopy. Int Immunol 1990; 2: 113–25.

Thieben MJ, Lennon VA, Boeve BF, Aksamit AJ, Keegan M, Vernino S. Potentially reversible autoimmune limbic encephalitis with neuronal potassium channel antibody. Neurology 2004; 62: 1177–82.

Tüzün E, Dalmau J. Limbic encephalitis and variants: classification, diagnosis and treatment. Neurologist 2007; 13: 261–71.

Tüzün E, Zhou L, Baehring JM, Bannykh S, Rosenfeld MR, Dalmau J. Evidence for antibody-mediated pathogenesis in anti-NMDAR encephalitis associated with ovarian teratoma. Acta Neuropathol 2009; 118: 737–43.

Vedeler CA, Antoine JC, Giometto B, Graus F, Grisold W, Hart IK, et al. Management of paraneoplastic neurological syndromes: report of an EFNS Task Force. Eur J Neurol 2006; 13: 682–90.

Viglietta V, Kent SC, Orban T, Hafler DA. GAD65-reactive T cells are activated in patients with autoimmune type 1a diabetes. J Clin Invest 2002; 109: 895–903.

Vincent A, Buckley C, Schott JM, Baker I, Dewar BK, Detert N, et al. Potassium channel antibody-associated encephalopathy: a potentially immunotherapy-responsive form of limbic encephalitis. Brain 2004; 127: 701–12.

Vincent A, Irani SR, Lang B. The growing recognition of immunotherapy-responsive seizure disorders with autoantibodies to specific neuronal proteins. Curr Opin Neurol 2010; 23: 144–50.

Vincent A, Lily O, Palace J. Pathogenic autoantibodies to neuronal proteins in neurological disorders. J Neuroimmunol 1999; 100: 169–80.

Warren JD, Scott G, Blumbergs PC, Thompson PD. Pathological evidence of encephalomyelitis in the stiff man syndrome with anti-GAD antibodies. J Clin Neurosci 2002; 9: 328–9.

Wieser HG, ILAE commission on neurosurgery for epilepsy, ILAE commission report: Mesial temporal lobe epilepsy with hippocampal sclerosis. Epilepsia 2004; 45: 695–714.